The PARET Code and the Analysis of the SPERT I Transients

William L. Woodruff

Argonne National Laboratory

Introduction

The PARET code[1] has been adapted for the testing of methods and models and for subsequent use in the analysis of transient behavior in research reactors. Comparisons with the experimental results from the SPERT-I transients[2,3] are provided. The code has also been applied to the analysis of the IAEA 10 MW benchmark cores for protected and unprotected transients.[4,5]

The PARET code was originally developed for the analysis of the SPERT-III experiments for temperatures and pressures typical of power reactors. This code has now been modified to include a selection of flow instability, departure from nucleate boiling (DNB), single and two-phase heat transfer correlations, and a properties library considered more applicable to the low pressures, temperatures, and flow rates encountered in research reactors. The PARET code provides a coupled thermal, hydraulic, and point kinetics capability with continuous reactivity feedback, and an optional voiding model which estimates the voiding produced by subcooled boiling.

The present version of the PARET code provides a convenient means of assessing the various models and correlations proposed for use in the analysis of research reactor behavior. For comparison with experiments the SPERT-I cores B-24/32, B-12/64, and D-12/25 were chosen. The B-24/32 core is similar in design to many plate type research reactors in current operation, and the D-12/25 core is of interest because the test included both nondestructive and destructive transients.

The PARET Code and Modifications

The PARET code provides a coupled thermal, hydrodynamic, and point kinetics capability. The core can be represented by one to four regions. Each region may have different power generation, coolant mass flow rate, and hydraulic parameters as represented by a single fuel pin or plate with its associated coolant channel. The heat transfer in each fuel element is computed on the basis of a one-dimensional conduction solution in each of up to 21 axial sections. The hydrodynamics solution is also one-dimensional for each channel at each time node. The heat transfer may take place by natural or forced convection, nucleate, transition, or stable film boiling, and the coolant is allowed to range from subcooled liquid, through the two-phase regime, and up to and including super-heated steam and allows for coolant flow reversal. The code also has an optional "voiding model" which estimates the voiding produced by subcooled boiling.

A modified Runge-Kutta method is used for the solution of the point kinetics equations. The solution may include up to 15 groups of delayed neutron data. Axial power distribtuions may be specified for each representative region. The externally inserted reactivity may be specified as a function of time, and feedback reactivity accounts for the effects of changes in

fuel temperature, linear thermal expansion, and initially only the moderator density (changes with the moderator temperature were not explicitly included). The code has now been modified to include a moderator temperature (spectrum) component, as well as, a void/density component. Separate coefficients and axial distributions for the fuel temperature, moderator temperature, and void/density components may be specified for each of the regions represented. The total reactivity feedback is a volume weighted sum of the pointwise contributions.

The heat transfer solution is obtained at each axial segment for each region represented. Each representative fuel element (region) may be subdivided into a maximum of 43 sections over a maximum of three zones (fuel, gap, and clad). The zones are characterized by their temperature dependent thermal conductivity and volumetric heat capacity. The coolant at each axial segment is represented by a bulk temperature and average coolant properties. The heat transfer at the clad-coolant interface is determined by the heat transfer correlation selection and the local flow regime.

The hydrodynamic solution in the code is based on a modified Momentum Integrated Model (MIM). The conservation equations are expressed as

$$\frac{\partial \bar{\rho}}{\partial t} = - \frac{\partial G}{\partial z} \tag{1}$$

$$\frac{\partial G}{\partial t} + \frac{\partial}{\partial z}\left(\frac{G^2}{\rho'}\right) = - \frac{\partial P}{\partial z} - \left(\frac{f}{\rho}\right)\left(\frac{|G|G}{2D_e}\right) - \bar{\rho} g \tag{2}$$

$$\rho'' \frac{\partial E}{\partial t} + G \frac{\partial E}{\partial z} = q \tag{3}$$

where

G = mass flow rate

P = pressure

E = enthalpy

f = friction factor

g = gravitational acceleration

q = heat source per unit volume

with

$$\bar{\rho} = \rho_\ell (1 - \alpha) + \rho_v \alpha \qquad \text{Average density}$$

$$\frac{1}{\rho'} = (1 - \chi)^2/[\rho_\ell (1 - \alpha)] + \chi^2/(\rho_v \alpha) \qquad \text{Momentum density}$$

and $$\rho'' = [\rho_\ell \chi + \rho_v (1 - \chi)] \frac{\partial \alpha}{\partial \chi} \qquad \text{Slip flow density}$$

where

ρ_ℓ and ρ_v are the saturated liquid and vapor densities, respectively, at some reference pressure.

α = vapor volume fraction (void fraction)

χ = vapor weight fraction (quality)

In Eq. (3) the pressure change terms

$$\frac{\partial P}{\partial t} + \left(\frac{G}{\rho}\right) \frac{\partial P}{\partial z}$$

and the dissipation term

$$\frac{f}{\rho} |G| G^2 / 2\rho D_e$$

are neglected.

The basic assumptions[6] of the MIM are 1) a channel averaged mass flow rated can be used for the momemtum equation, Eq. (2), with

$$\overline{G} = \frac{1}{L} \int_0^L G \, dz \quad \text{for channel length L,}$$

and 2) all coolant properties are independent of pressure and evaluated at some reference pressure. In the modified MIM for PARET, the coolant density is evaluated as a function of the localized pressure, while all other coolant properties are functions of temperature only. The local density also depends on the voiding predicted (the voiding model option is discussed in a later section).

The code system includes an extensive coolant properties library. This library is used to generate internal tables at a specified reference pressure. The code uses a table look up to evaluate local coolant properties. The code was originally developed at the Idaho Natonal Engineering Laboratory to analyze the SPERT-III experiments with temperatures and pressures typical of power reactors. Thus, the original properties library covered a broad range of temperatures and pressures with little detail over the range of interest to research reactors. A revised properties library has been generated for the analysis of research reactors. Only properties for light water applications are available.

The code has been modified to include a selection of flow instability and DNB correlations applicable to the low pressure regimes typical of research reactors, and the McAdams and Bergles-Rohsenow (B-R) two-phase correlations have been added as options to the original Jens-Lottes (J-L) correlation. A transition model from the onset of nucleate boiling (ONB) to fully developed nucleate boiling is also now available on option. Either the original Dittus-Boelter (D-B) correlation or the Sieder-Tate (S-T) correlation may now be used

for the single-phase, subcooled forced convection regime. The code also now includes a model for predicting the decay heat power based on the ANS curve for fission product decay heat, a model for simulating control insertion with trip settings for overpower and low flow, enhancements in the data available for edits, and a plot file summary. The code provides edits of the elapsed time, power, energy release, period, reactivity, mass flow rate, heat flux, burnout ratio, local pressure, and temperatures at each (or selected) time steps and writes selected data at each time step to a summary file for subsequent processing or plotting.

The SPERT I Experiments

The SPERT program was initiated in 1954. The purpose of the program was to obtain a better understanding of the behavior of nuclear reactors under transient conditions. The tests included a variety of configurations under a broad range of conditions up to and including destructive tests.

The tests on highly enriched uranium, plate-type fuel in the SPERT I series are well suited to the purpose of this study. The SPERT I facility consisted of an open tank of light water into which various core configurations could be assembled. This facility had no provisions for pressurization or forced cooling. The water level over each core was maintained at a height of 61 cm (2 ft). In the B-cores the fuel assemblies provided for the removal of selected fuel plates, and a variety of core characteristics were achieved. The experiments covered a wide range of transients characterized by the initial period or inverse period induced by a step insertion of reactivity. The measurements included reactor power, plate surface temperature, and pressure. Tests in the SPERT I facility ended with destructive tests on the D-12/25 core in November of 1962.

Two SPERT I cores in the B-series and the D-12/25 core were selected for these comparisons. The characteristics and kinetics parameters for these cores are provided in Table I. The B-24/32 core with 24 fuel plates/element and 32 elements is quite similar in design to many plate type research reactors in current operation. The 12 plate/element B-12/64 core has larger water channels and a much smaller void reactivity coefficient. These two choices of SPERT I B-cores cover a range of temperature and void reactivity coefficients. The D-12/25 SPERT I core includes both nondestructive and destructive transients for comparison.

With the exception of the void reactivity coefficient for the B-12/64 core, the kinetics parameters for the SPERT I cores are data obtained by Clancy et al.[7] from perturbation theory computations. The experimental values quoted for the temperature reactivity coefficients are not considered appropriate for the analysis of fast transients. As noted in Ref. 7, these measurements were made by uniformly heating the coolant in the reflector as well as the core, and a significantly lower coefficient is obtained due to the positive component from the reflector. The temperature of the coolant in the reflector would not change during the transients considered in this comparison. The other coefficients computed from the perturbation theory model generally agree well with the experimental values. The void reactivity coefficient computed for the B-12/64 core, however, is only about half the value determined from the experiments. Thus, the quoted experimental coefficient has been used for this core.

The PARET Models and Correlation Selections

Many attempts have been made to develop models which predict the SPERT results. Forbes et al.[8] used various empirical models based on modifications of the Fuchs model with some degree of success. The work of Turner[9] included expressions for the heat transfer rate and void formation with fitted coefficients and was only moderately successful in predicting the experimental results. These empirical and fitted models give little insight into which physical properties and feedback mechanisms are important in describing the behavior of a reactor under transient conditions. Clancy et al.[7,10] used a "boiling" model which neglects any explicit voiding contributions. This model has been quite successful in predicting a wide range of transients but has had some difficulties when substantial voiding is expected.

The PARET code provides for feedback from coolant temperature changes, the expansion of the fuel plates with temperature, the Doppler, and changes in the density of the coolant with temperature and with voiding. Voiding may occur as a result of bulk boiling of the coolant or from the optional voiding model for subcooled boiling. Thus, all of the major feedback mechanisms are included, and separate reactivity coefficients may be assigned for each component. The reactivity coefficients for each SPERT core were taken as those specified in Table I. The Doppler coefficient was neglected in these fully enriched uranium cores. A uniform axial weighting was assumed for each coefficient.

A two channel model was used in the PARET code with one channel representing the hottest fuel plate in the core and the second channel representing the remainder of the core. For the second, "average," channel a cosine distribution was assumed for the axial power shape with a peak of 1.311 corresponding to the buckling used in computing the reactivity coefficients. The overall peak/average as quoted in Table I was applied for the hot channel. The axial dimension for each channel was divided into 21 equally spaced nodes over the active core region, and the fuel and clad regions were assigned 5 and 2 nodes, respectively, for the radial heat transfer solution. While the PARET code provides the capability for an accurate description of the inlet and outlet plenum regions, sufficient details were not available for this purpose. The inlet plenum length was specified as 0.0 cm, and an outlet plenum length of 61.0 cm (24 in) was specified corresponding to the water level over the core region. The nominal pressure is specified at the plenum outlet as atmospheric pressure. The inlet and exit loss coefficients were set at 0.55 and 0.65, respectively. A flow-forced problem was specified with an initial inlet flow rate of 0.3 cm/s to simulate natural convection. All transients were initiated from a power level of 5W, an inlet temperature of 20°C, and with a ramp insertion of reactivity to 70 ms (approximate step).

The PARET results over the range of transients covered by the SPERT I experiments have been found to be relatively insensitive to the choice of plenum model and loss coefficients (only the friction pressure drop across the plenum is affected), the inlet coolant flow rate, and the reactivity insertion ramp rate. The results are somewhat more sensitive to the choice of parameters chosen for the void model used in PARET and strongly dependent on the choice of heat transfer correlations with both single and two phase flow. There has long been a concern about the applicability of steady-state correlations for the analysis of reactors under transient conditions. There is also still uncertainty about which feedback mechanism is dominant in limiting the transient when subcooled boiling is present. The choice for a best model or a best set of correlations, at this time, is not clear, and one of the purposes of this comparison is to see if a preferred choice can be determined.

Table I. Core Characteristics and Parameters

Parameter	SPERT I		
	B-24/32	B-12/64	D-12/25
Plates/Element, Std. (Contl.)	24	12	12(6)
Number of Elements, Std. (Contl.)	32	64	20(5)
Fuel Thickness, cm	0.051	0.051	0.051
Clad Thickness, cm	0.051	0.051	0.051
Water Channel, cm	0.165	0.483	0.455
^{235}U/plate, g	7.0	7.0	14.0
Temperature (spectrum)* Coeff., $/°C	-2.528-2	-4.157-2	-2.801-2
Void Coefficient, $/% Void	-0.3571	-0.150	-0.4214
Neutron Generation Time, μs	50.0	77.0	60.0
βeff	0.007	0.007	0.007
Peak/Ave. Power	2.5	2.2	2.4

*The Doppler Coefficient is negligible for all cases.

The PARET code includes an optional voiding model for subcooled boiling of the form

$$\frac{\partial \alpha}{\partial t} = \lambda K(q")^n - \frac{\alpha}{\tau} - Cv \frac{\partial \alpha}{\partial z} , \qquad (4)$$

where

α = the void fraction at axial location z and time t

λ = the fraction of the surface heat flux producing voids

K = a constant at a given operating pressure

q" = the heat flux at axial location z and time t

n = the source exponent

τ = the bubble life time

C = the flow distribution parameter

and v = the flow velocity of the coolant.

The void fraction impacts the modified MIM solution, Eqs. (1) - (3), through the local density. This model and variants of this model along with some of the experimental work on void formation are discussed by Morgan.[11] The terms λ, n, τ, and C are adjustable parameters (input to PARET) dependent on the degree of subcooling. The value of n is generally taken as 1.0. The fraction of the heat flux contributing to the generation of voids, λ, varies with pressure in the range from 0-0.4, however, a value of 0.05 has been suggested from the SPERT III tests. The bubble life time, τ, from experiments should range from ~100 μs for highly subcooled regions where bubble collapse is rapid to an infinite value with bubbly flow. Finally, for the parameter C a value of 0.8 is recommended for the highly subcooled region where bubbles do not detach from the surface but move at about 80% of the coolant velocity along the surface, and a value of 1.13 is suggested for slightly subcooled regions where vapor velocity exceeds the coolant velocity with bubbly flow. The suggested values from the SPERT III experiments of n = 1.0, λ = 0.05, τ = 0.001s, and C = 0.8 were initially tested in this analysis. Values for λ and τ must be specified in PARET for both the nucleate boiling and transition boiling regimes, and a value for λ must be input for film boiling. The transition and film boiling parameters were set to the suggested values and remained fixed.

In preliminary studies with no subcooled boiling it was apparent that the existing heat transfer correlation for natural convection (Reynolds number, Re, ≤2000) was inadequate, and that the heat transfer coefficient was too low. Thus, the single phase heat transfer model in PARET was revised to incorporate an approximation of the heat transfer coefficient proposed by Rosenthal and Miller[12] as

$$h = \sqrt{\frac{k \rho C_p}{T}} ,$$

where

h = the heat transfer coefficient at the clad-coolant interface

k = the thermal conductivity of the coolant

ρ = the density of the coolant

C_p = the specific heat of the coolant

and T = the period of the power rise

This expression is based on the analysis of transient experiments in which the power in an electrically heated ribbon was increased exponentially as e^{t}/T with time, t, and should be valid for $t > T$. This coefficient may now be used with both natural and forced convection if the value is larger than the original heat transfer coefficient for $Re < 2000$, and if this coefficient is larger than that computed for the chosen forced convection correlation with $Re > 2000$. The use of this method requires the selection of an appropriate period. In the current version of PARET, T is chosen as the minimum T_m such that $|T_m - T_{m-1}|/T_{m-1}$ is less than 0.01, where T_m is the instantaneous period at time step m. This has proven to be a reasonable criterion under most conditions.

Preliminary studies have also shown that the ONB is best predicted by the B-R correlation, and that the McAdams and J-L correlations are better choices for fully developed nucleate boiling conditions. The transition model for two phase flow must then be chosen over the original scheme to provide the B-R correlation for ONB while allowing fully developed nucleate boiling to be described by either the McAdams or the J-L correlation. These two choices for fully developed nucleate boiling give approximately the same results as long as the subcooled boiling regime is restricted to nucleate boiling.

If transition boiling is predicted, the results will depend on not only which two phase correlation was selected but on the choice of correlations selected for predicting a critical heat flux as well. The two phase correlation selected for nucleate boiling is also used to estimate the critical temperature corresponding to the computed critical heat flux. If the current clad surface temperature is greater than this estimated critical temperature but less than or equal to the temperature for departure from transition boiling, then transition boiling is predicted. The predicted temperature for departure from transition boiling is likewise dependent on the critical heat flux and the corresponding temperature.

Implicit in this formulation is the assumption that the critical heat flux is also the DNB heat flux. This may or may not be the case. It appears that some choices of correlations for two phase and critical heat flux are overly conservative and prematurely predict film boiling for some transients. Thus, the McAdams two phase correlation and the original DNB correlation for critical heat flux were found to give the most realistic estimates for the more energetic transients. These predictions for early transition boiling and finally film boiling may still be questioned.

Results

The "best" model for the PARET code consists of the use of the Rosenthal and Miller relation for the single phase heat transfer coefficient (at least at low flow rates), the McAdams correlation for fully developed two phase flow with the B-R correlation for ONB and transition to fully developed nucleate boiling, the original DNB correlation for critical heat flux estimates, and the voiding model as described earlier for the generation of voids with subcooled boiling. The model also includes feedback contributions from the radial expansion of the clad. Contributions to the feedback due to Doppler have been neglected. The results from the application of this model to the SPERT I B-24/32 and B-12/64 cores are shown in Figs. 1 and 2. These figures

FIGURE 1. SPERT I: B-24/32 Data and PARET Comparison

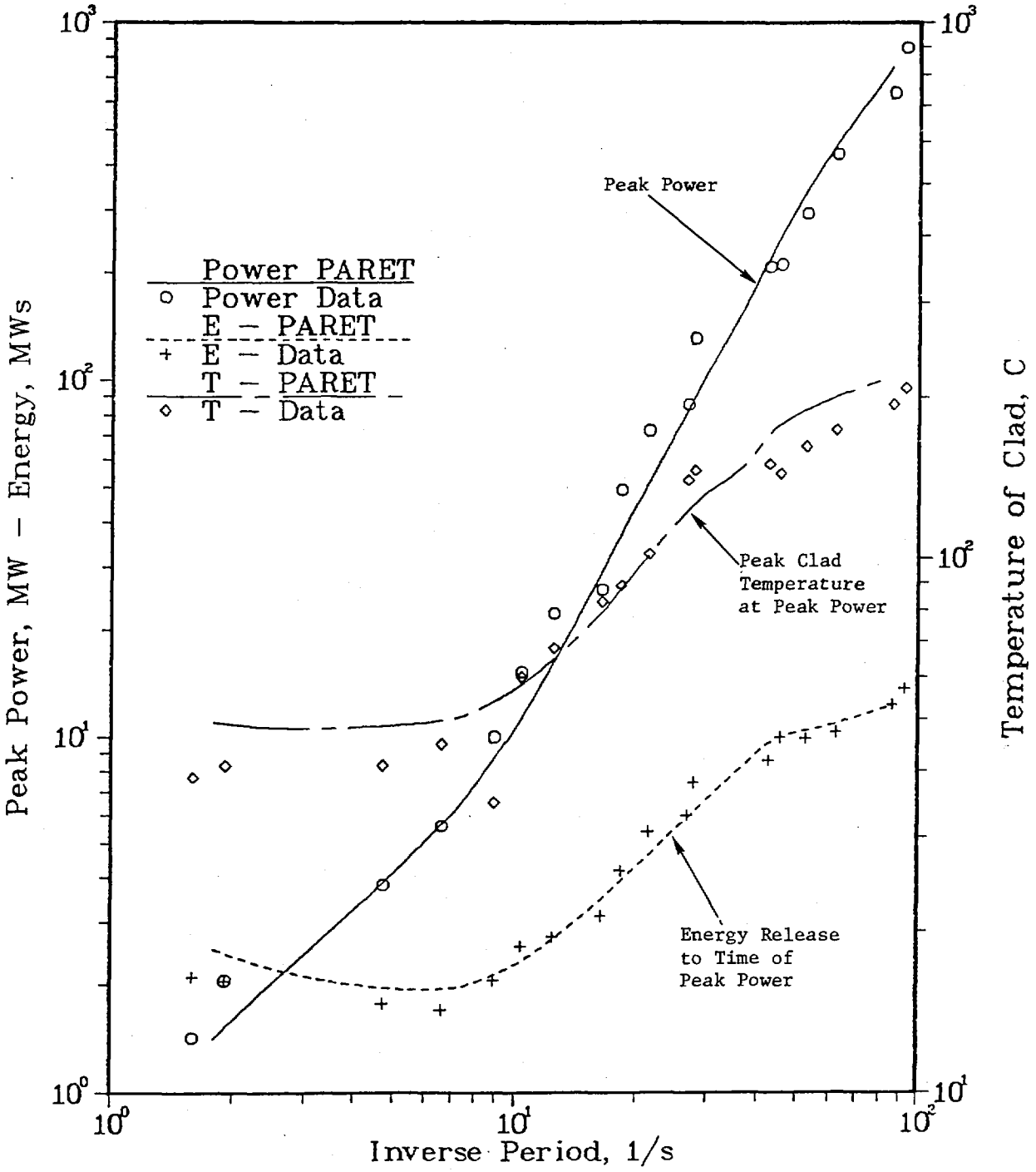

FIGURE 2. SPERT I: B-12/64 Data and PARET Comparison

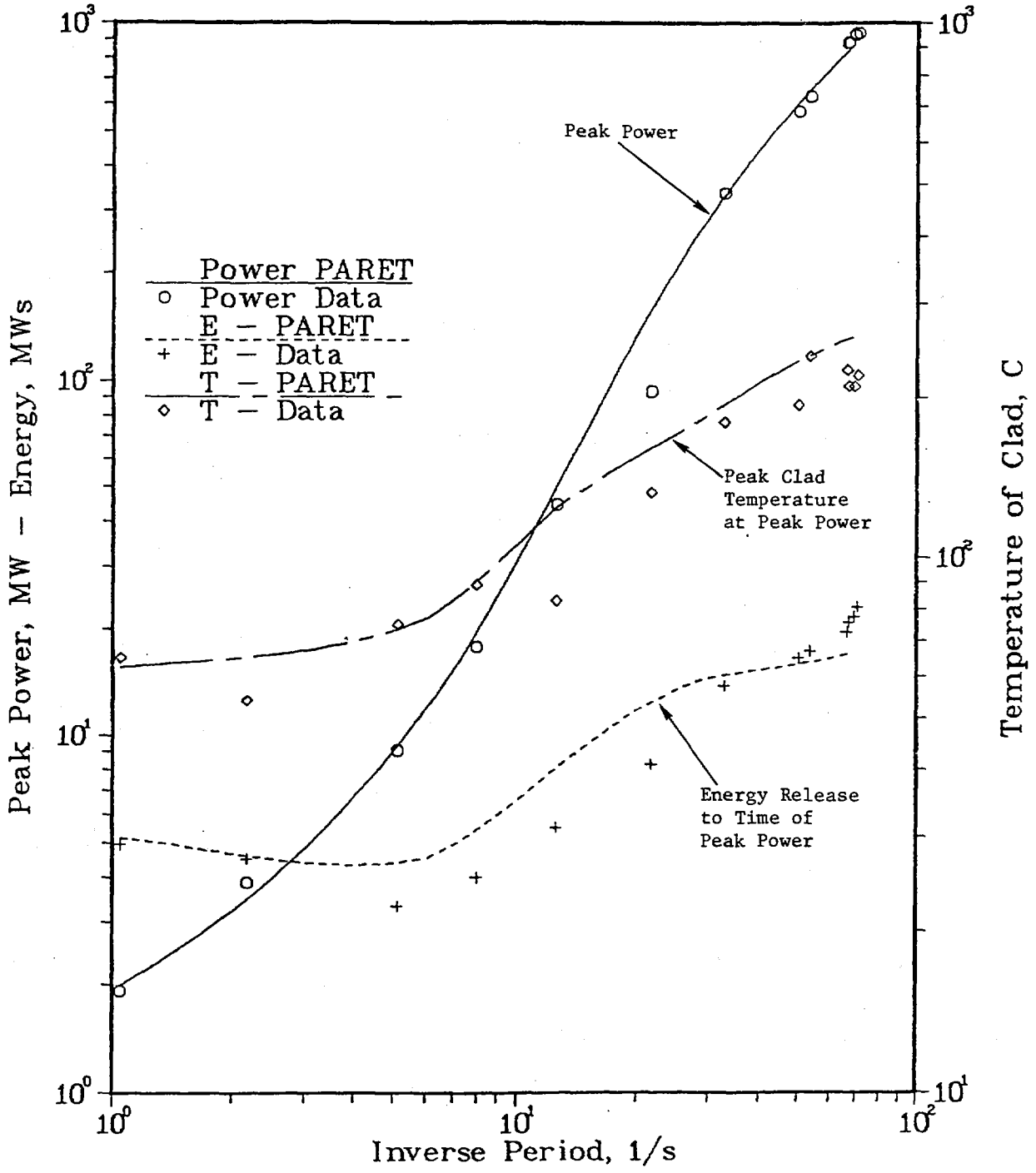

show the SPERT I experimental data points and the PARET computed results for the peak power, the energy release to the time of peak power, and the peak clad temperature at the time of peak power as a function of the inverse period. The PARET results generally agree quite well with the experimental data.

The B-24/32 core has the larger void reactivity coefficient of the two B cores considered and a smaller temperature coefficient. The PARET code predicts the onset of nucleate boiling in the average channel at an inverse period of about $44s^{-1}$. This agrees well with what the SPERT I data show. The effects of enchanced two phase heat transfer are most evident in the energy release data (see Fig. 1). These data show an inflection and a subsequent plateau for inverse periods larger than $\sim 40s^{-1}$. The clad temperature data show a similar trend, although the scatter of these data make this more difficult to see. The shape of the PARET curves agree well with the data. For inverse periods greater than about $44s^{-1}$ the dominant feedback component is due to voiding.

The energy release and clad temperature results are the most sensitive to the choice of parameters for the void generation model. The suggested parameters of $\lambda = 0.05$ and $\tau = 0.001s$ for Eq. (4) from the SPERT III analysis have been shown to give an energy release value which is about 7% too low while the clad temperature is about 7% lower than that shown for the largest inverse period computed. The results were insensitive to the choice for C (perhaps due to the low flow rate). The original PARET code contained only a void/density feedback coefficient, and the voiding model parameters determined from the SPERT III experiments may be suspect. The parameters used in this comparison are $\lambda = 0.03$ and $\tau = 0.0005s$ for the nucleate boiling regime. The larger heat flux fraction and the longer bubble life time from the SPERT III tests would give better agreement for clad temperature but somewhat poorer agreement for the energy release. The lower values used here give a conservative estimate for the clad temperature from a safety point of view.

The B-12/64 core has a very small void reactivity coefficient, but the temperature coefficient for the coolant is larger than that of the B-24/32 core. This is consistent with the large water channels for this case. With a small void reactivity coefficient one might expect that voiding would play a rather minor role, however, this is not the case. This core, as predicted by PARET, shows more extensive and more intensive subcooled boiling than the B-24/32 core. The code predicts the onset of nucleate boiling in the average channel for an inverse period of about $25s^{-1}$ and transition boiling for inverse periods greater than about $40s^{-1}$.

Transition boiling is predicted over about one third of the core for the most energetic transient. It is, of course, questionable that stable transition boiling actually occurred in the experiment. The code predicts transition boiling only because the conditions described earlier were satisfied. This suggests that this critical heat flux correlation is also probably too conservative to give agreement with experiment. Other correlations will even predict film boiling.

The agreement with experiment is quite good except for the energy release to peak power, and this somewhat poor agreement covers a range where no subcooled boiling is predicted. This is very similar to the disagreement observed by Clancy et al.[7] for this core. One can certainly not fault the

the voiding model for this disagreement. The voiding model does, however, impact the results for the more energetic transients, and the choice of the voiding parameters for transition boiling now must be considered. The values used for this comparison were $\lambda = 0.05$ and $\tau = 0.001$s with transition boiling and $\lambda = 0.03$ and $\tau = 0.0005$s, as before, with nucleate boiling. With a value of $\lambda = 0.03$ for transition boiling, the energy release to peak power for the most energetic transient increases by 13% to 19.4 MWs and agrees well with the experimental data. The clad temperature, however, increases by 15%, and the peak clad temperature at peak power is further over-estimated.

The D-12/25 SPERT I core provides data which include destructive tests. The tests are reported to show stuctural damage to the plates, rippling and bowing due to thermal stresses, for periods ~7 ms, and several plates melted at the core center for periods ~5 ms. While the exact onset of clad melting was not determined, the onset is in the range $5.0 < T < 6.0$ ms. The last test with a period of 3.2 ms resulted in melting of ~35% of the fuel and severe damage to the core and structurals. The SPERT results for peak power, energy release to peak power, and the clad temperature at peak power are shown in Fig. 3 along with the results computed by PARET. The PARET results for the D-12/25 core show good agreement over the range of short periods where core damage (inverse period $\alpha_o \sim 140s^{-1}$, $\Delta\rho \sim \$2.16$) and melting ($\alpha_o > 166s^{-1}$, $\Delta\rho \sim \$2.36$) were reported. The code also showed that the clad surface temperature in the hot channel exceeds the melting point for the clad (582°C) with a \$2.30 insertion and a period of 6.6 ms ($\alpha_o \approx 152s^{-1}$). Thus, the PARET code gives a slightly conservative estimate for onset of clad melting compared with experiment.

The D-12/25 core estimates, like the B-12/64 core, show somewhat poorer agreement for clad temperature and energy release over the range of transients where no voiding is predicted. This suggests that either the single phase heat transfer rate to the coolant is too small or the coolant temperature coefficient for feedback is too low. The usual application of steady-state correlations for the analysis of transients is an open question, and more experimental data is needed in this area. The applicability of isothermal and uniformly weighted temperature feedback coefficients is likewise questionable for transient analysis. From a safety standpoint, however, the errors introduced appear to be on the side of conservatism. At the higher reactivity insertions, where subcooled boiling is predicted, feedback from the void/density component clearly dominates. Feedback from changes in the coolant temperature are only a few percent of the total, and feedback due to expansion of the fuel plate is an even smaller component.

DNB and the onset of film boiling does not necessarily result in "burnout" or critical heat flux conditions. With a \$2.00 insertion ($\alpha_o \sim 118s^{-1}$) in the D-12/25 core, for example, the code predicts film boiling, but the clad temperature does not reach the melting point. The peak fuel meat temperature never exceeds the melting point of the clad. Thus, even with the poor heat transfer of film boiling the clad temperatue can never reach the melting point.

As already noted, many critical heat flux correlations are overly conservative. This is particularly true with the use of flow instability correlations. These correlations may not be applicable to transient conditions. Flow instability conditions have not been noted as a difficulty in the SPERT test.

FIGURE 3. SPERT I: D-12/25 Data and PARET Comparison

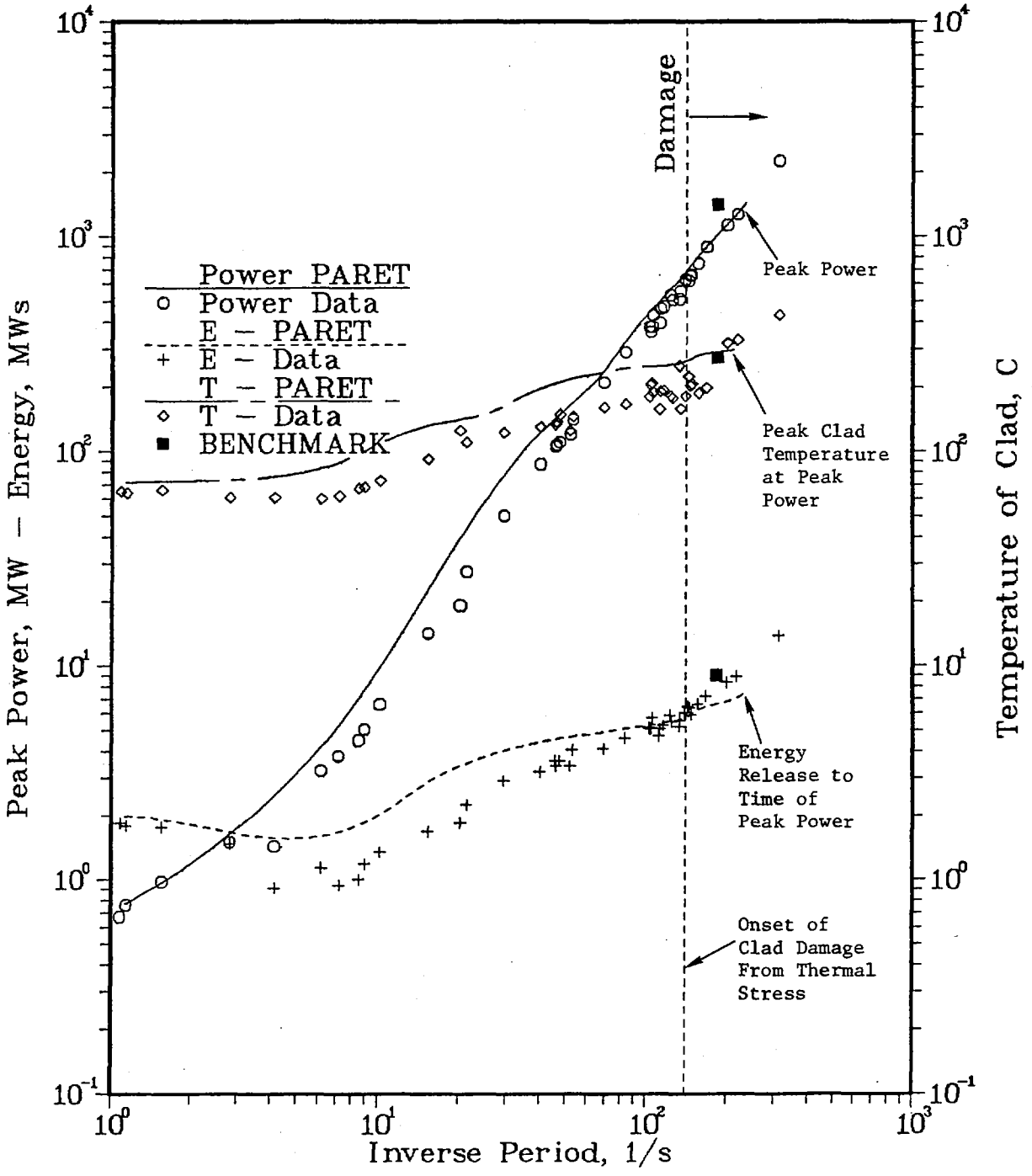

Only modest pressure pulses are reported in all but the final destructive test. The code, however, predicts stronger changes in pressure and flow with subcooled boiling including flow reversal in some cases. In the more extreme transients the code shows a series of setbacks in the clad temperature associated with partial collapses in the film boiling and voiding. The experimental data[3] show a similar structure in the clad surface temperature measurements. These data are considered unreliable at the higher temperatures,[13] and no attempt is made to compare results. It is also difficult to separate and assess the influence of limitations in the methods and code instabilities on the PARET results. In spite of some questions of detail, the code predicts the onset of clad melting in good agreement with experiment.

While no attempt has been made to assign experimental uncertainties to the SPERT I data, the measured temperatures would probably have the highest degree of uncertainty. The reported values were taken from different thermocouples and from slightly different locations in the core. Also, any delays in response time would tend to show a lower temperature. Overall the agreement for the clad temperature should be considered quite good.

Application to Research Reactors

The IAEA 10 MW benchmark core[4] has been selected here as typical of a large class of research reactors. The specifications include a highly enriched uranium (HEU) core and low enrichment (<20%) uranium (LEU) core. These cores have been used as benchmarks for the transient analysis of research reactors.[5] The detailed specifications are given in Refs. 4 and 5, and the results for the specified benchmarks using the PARET code are provided in Ref. 5. Although the transients specified for the benchmark cores did not include self-limiting cases, it is of interest to consider such cases, and the limits imposed on reactivity insertions by the clad melting temperature.

The PARET options and parameters used here are identical to those derived from the SPERT I comparisons. These options now include the S-T correlation for forced convection single phase flow. Based on the favorable results from the SPERT I comparisons, this model should give reasonable estimates for the peak clad temperature for the benchmark cores. The clad melting temperature is again taken as 582°C for 6061 alloy.

Table II provides a comparison of both the HEU and LEU benchmark cores for both protected and unprotected transients of \$1.50/0.5s. This table also provides a comparison of some of the reactivity feedback coefficients and parameters for the HEU and LEU cases. Uniform (isothermal) coefficients with a uniform weighting were assumed. The prompt neutron generation time, Λ, and the Doppler coefficient show the largest changes with enrichment, and these differences are largely responsible for the observed differences in the transient results.

The influence of the larger Doppler coefficient for the LEU core in the cases with scram is overshadowed by the negative reactivity from the insertion of control rods. The shorter Λ for the LEU core produces a smaller initial period and a faster rise in power. Consequently, the LEU case with scram shows a slightly higher peak power than the HEU case. In the unprotected (self-limited) transients, the strong influence of the large Doppler feedback in the LEU cases is quite apparent. All of the values recorded are substantially lower for this LEU case. The larger void/density coefficient with LEU also contributes to the differences noted. The prompt Doppler feedback in the LEU case dominates during the early stages of the transient. The LEU case without Doppler feedback is also shown, and without the Doppler contribution the transient response is substantially worse.

Table II. $1.50/0.5s Benchmark Cases with and Without Scram

Case		Period, ms	$\hat{P}$, MW (t_m, s)	E_{t_m}, MWs	$\hat{T}_{clad}$, °C at t_m	$\hat{T}_{clad}$, °C Max. (t, s)
HEU	With Specified Scram	14.5	132 (0.656)	3.29	131	156 (0.672)
	Self-limited	14.5	371 (0.667)	7.30	220	308 (0.685)
LEU	With Specified Scram	11.9	146 (0.613)	2.94	126	157 (0.628)
	Self-limited	11.9	283 (0.622)	5.56	181	263 (0.642)
	Self-limited (no Doppler)	11.9	445 (0.621)	6.87	220	314 (0.636)

Reactivity Coefficients and Parameters

	Λ, μs	β_{eff}	Coolant Temperature $/°C	Void/density, $/% Void	Doppler, $/°C
HEU	55.96	7.607-3	1.537-2	0.3257	3.6-5
LEU	43.74	7.275-3	1.082-2	0.4047	3.31-3

The PARET code has also been used to determine the reactivity insertion limits imposed by the clad melting temperature. For the HEU benchmark core, a step insertion of ~$2.35 is the limiting case, i.e. for reactivity insertions larger than this limit the peak surface temperature of the clad is predicted to exceed the clad melting temperature. The results from the $2.35 step at the time of peak power are compared with results obtained for the SPERT I D-12/25 core Fig. 3 The agreement with experiment is remarkably good even though the two cores have quite different characteristics. This simularity of behavior was also noted in the diversity of cores considered in the SPERT I series of experiments.[8] The threshold for clad melting can serve as a useful indicator for the limits on reactivity insertions.

Figure 4 provides a comparison of the HEU and LEU benchmark cores showing the clad melting threshold for reactivity insertions over a range of ramp durations (from a step to 0.75s). The areas above the curves indicate where clad melting would be expected. Also shown in this figure is the corresponding maximum net reactivity inserted (the difference between the external reactivity inserted and the reactivity from feedback). This maximum generally occurs at the same time in the transient as the minimum period.

While the two curves in Fig. 4 for HEU and LEU fuel show some similarities, they also show some substantial differences. The LEU core can clearly tolerate a larger reactivity insertion before clad melting than the HEU core. The maximum step insertion is ~$2.80 for the LEU core compared to ~$2.35 for the HEU core. Both curves show the same general shape. The ramp insertions of short duration are equivalent to a step insertion. The entire ramp is inserted before the power, temperatures, and feedback have increased substantially, and the limiting reactivity insertion remains constant. For ramps of longer duration, the feedback reactivity limits the net reactivity and turns over the transient before the maximum of the ramp is reached. A limiting ramp rate (constant slope) is reached, and a constant maximum net reactivity is observed for each case. The limiting ramp rate for the LEU core, ~14.8 $/s, is more than double that for the HEU core, ~6.4 $/s. The LEU core also shows an earlier transition from the limiting step portion of the curve to the limiting ramp rate range.

Table III shows the limiting cases for LEU with a 0.5s ramp as the Doppler and the larger void coefficient are eliminated to approximate the HEU case. The Doppler contributes about 2/3 of the difference noted between the LEU and the HEU limits, the larger void coefficient contributes another 28% of the difference, and the remaining ~5% difference can be attributed to other unresolved differences such as the prompt neutron generation time, for example. The benefits of a prompt Doppler coefficient with LEU fuel are clearly demonstrated by these results.

Conclusions

The results of this comparison of the PARET code with the SPERT I cores are generally quite favorable. The agreement with the B-24/32 core is particularly good. This core might be considered a more representative core for research reactors than either the B-12/64 or D-12/25 cores. These results

Table III. Feedback Components with 0.5s Limiting Ramp

Case	Limiting Ramp, $	Relative Change (% of Total)
LEU Base	7.40	-
LEU without Doppler	4.60	-2.80 (67)
LEU without Doppler and with HEU void Coefficient	3.40	-4.00 (95)
HEU	3.20	-4.20 (100)

Figure 4. Reactivity Insertion Limits for Clad Melting

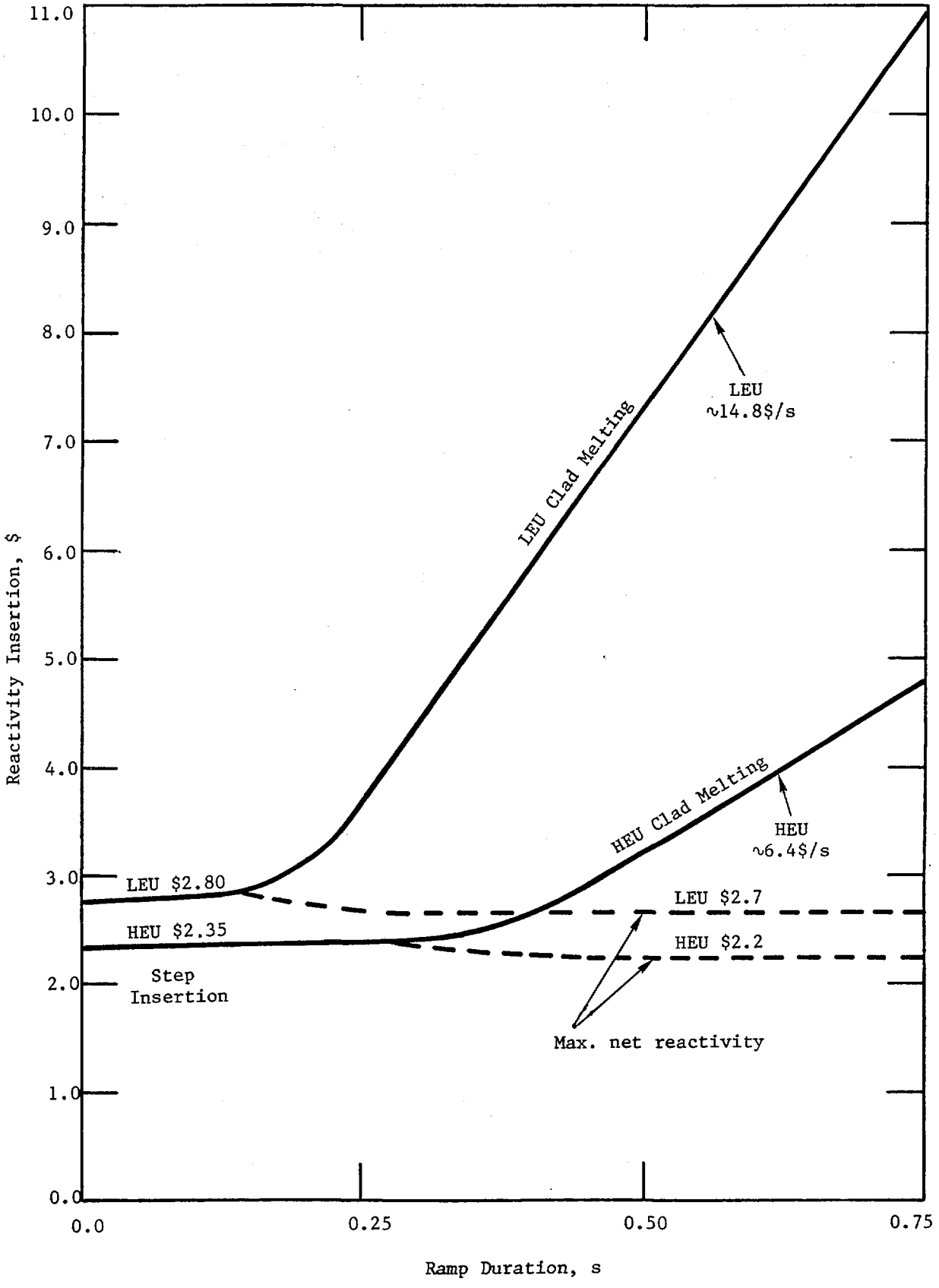

have demonstrated that the voiding model in the code can successfully describe the behavior of transients with subcooled boiling, and that certain choices of methods and correlations are preferred. It would appear that many steady-state critical heat flux correlations are too conservative for use in the analysis of transients. Finally, the code seems to provide conservative estimates for the peak clad temperature with the more energetic transients, and the limiting reactivity insertion cases (clad melting) can be determined.

The limiting clad temperature for the 10 MW HEU benchmark core agrees exceptionally well with the SPERT I data for a step insertion. The LEU benchmark core can withstand a substantially larger reactivity insertion without clad melting compared to the HEU core. The prompt Doppler coefficient with the LEU fuel is shown to be the major contributor to this improved behavior.

Acknowledgements

The author is grateful to Dr. James E. Matos for the many helpful suggestions and useful discussions throughout the course of this work.

References

1. C. F. Obenchain, "PARET - A Program for the Analysis of Reactor Transients," IDO-17282 (1969).

2. A. P. Wing, "Transient Tests of the Fully Enriched, Aluminum Plate-Type, B Cores in the SPERT I Reactor," IDO-16964 (1964).

3. M. R. Zeissler, "Non-destructive and Destructive Transient Tests of the SPERT I-D, Fully Enriched, Aluminum Plate-type Cores: Data Summary Report," IDO-16886 (1963).

4. "Research Reactor Core Conversion from the Use of Highly Enriched Uranium to the Use of Low Enrichment Uranium Fuels Guidebook," IAEA-TECDOC-233 (1980).

5. "Research Reactor Core Conversion from the Use of Highly Enriched Uranium to the Use of Low Enrichment Uranium Fuels Guidebook, Safety and Licensing Issues," IAEA, to be published.

6. J. E. Meyer, "Hydrodynamic Models for the Treatment of Reactor Thermal Transients," Nucl. Sci. and Eng., 10, 269 (1961).

7. B. E. Clancy, J. W. Connolly, and B. V. Harrington, "An Analysis of Power Transients Observed in SPERT I Reactors. Part I: Transients in Aluminum Plate-type Reactors Initiated at Ambient Temperature," AAEC/E345 (1975).

8. S. G. Forbes, F. L. Bentzen, P. French, J. E. Grund, J. C. Haire, W. E. Nyer, and R. F. Walker, "Analysis of Self-shutdown Behavior in the SPERT I Reactor," IDO-16528 (1959).

9. W. J. Turner, "Calculation of SPERT Transients," J. Nucl. Energy, 22, 397 (1968).

10. B. E. Clancy, J. W. Connolly, and B. V. Harrington, "An Analysis of Power Transients Observed in SPERT I REACTORS. Part II: Dependence of Burst Parameters on Initial Temperature and Core Moderation," AAEC/E383 (1976).

11. R. P. Morgan, "A Review and Discussion of Literature Concerning Transient Heat Transfer and Steam Formation," IDO-17226 (1967).

12. M. W. Rosenthal and R. L. Miller, "An Experimental Study of Transient Boiling," ORNL-2294 (1957).

13. J. E. Houghtaling, Alain Sola, and A. H. Spano, "Transient Temperature Distributions in the SPERT I D-12/25 Fuel Plates During Short-period Power Excursions," IDO-16884 (1964).